Development of an HPLC/UV assay for the evaluation of inhibitors of human recombinant monoacylglycerol lipase

S. Del Carlo,[a] C. Manera,[a]* A. Chicca,[b]* C. Arena,[a] S. Bertini,[a] S. Burgalassi,[a] S. Tampucci,[a] J. Gertsch,[b] M. Macchia,[a] G. Saccomanni[a]

[a]*Dipartimento di Farmacia, Via Bonanno 6, 56126 Pisa, Italy*

[b]*Institute of Biochemistry and Molecular Medicine, National Center of Competence in Research TransCure, University of Bern, CH 3012 Bern, Switzerland*

*To whom correspondence should be addressed. C.M.: *email address*: clementina.manera@farm.unipi.it; telephone: +39(0)502219548; fax: +39(0)502219605;. A.C. *e-mail address*: andrea.chicca@ibmm.unibe.ch; telephone: +41(0)316314125.

Abstract

Monoacylglycerol lipase (MAGL) is a membrane-associated cytosolic serine hydrolase which catalyses the hydrolysis of the endocannabinoid 2-arachidonoylglycerol into arachidonic acid and glycerol. MAGL represents the link between the endocannabinoid and the eicosanoid system indeed its inhibition enhances endocannabinoid signalling and lowers eicosanoid production. Here we present a radioactive-free, sensitive and solid HPLC-UV based method to evaluate MAGL activity by using 4-nitrophenylacetate (4-NPA) as substrate. The enzymatic activity is measured by quantifying the 4-nitrophenol (PNP) (λ=315 nm) formation on a C18 stationary phase. The method was validated by calculating IC_{50} values of the reference inhibitors JZL184, CAY10499 and JW642 and confirming the irreversible and non-competitive mechanism of inhibition for JZL184. Furthermore in order to resemble the catalytic conditions of MAGL at cell membrane level, the surfactant Triton® X-100 was added, as a micelle forming agent and 4-nitrophenyldodecanoate (4-NPDo) was used as lipophilic substrate for MAGL. The data obtained confirmed that the HPLC method is an alternative, radioactive-free approach for the screening and characterization of new MAGL inhibitors. Finally this assay prevents, in an unequivocal manner, any interference related to the intrinsic absorbance of screened compounds or metabolites generated upon enzymatic cleavage which could seriously affect the assay readout.

Keywords: HPLC-UV, MAGL, enzymatic assay, 4-nitrophenylacetate, 4-nitrophenyldodecanoate, 4-nitrophenol

1. Introduction

Monoacylglycerol lipase (MAGL) is a membrane-associated cytosolic serine hydrolase with the highest expression levels in the brain, white adipose tissue and liver [1]. MAGL catalyses the hydrolysis of monoacylglycerols into fatty acids and glycerol and the endocannabinoid 2-arachidonoylglycerol (2-AG) is one of its main substrates [2,3]. 2-AG is a lipid messenger which is synthesized on-demand from membrane phospholipid precursors and acts primarily by binding to cannabinoid G protein-coupled receptors (CB1R and CB2R). Recently it has also been shown that 2-AG can directly modulate GABA(A) receptor by behaving as a positive allosteric modulator [4]. In the brain, MAGL is responsible for about 80% of the hydrolysis of 2-AG while the remaining 20% occurs mainly from the activity of other two serine hydrolases, α,β-hydrolase-6 (ABHD-6) and -12 (ABHD-12) [5,6]. The pharmacological inhibition of MAGL activity *in vivo* leads to a strong accumulation of 2-AG, in particular in the brain which triggers a higher activation of CB1R and CB2R resulting in analgesic, anxiolytic, antidepressant, sleep-inducing and anti-inflammatory effects [7-10]. Recently, it has been shown that in some tissues, such as brain, liver and lung, 2-AG acts as a precursor for the arachidonic acid production [1]. Arachidonic acid is mainly oxygenated by cyclooxygenase-2 to generate pro-inflammatory eicosanoids such as prostaglandin-E2 and prostaglandin–D2. Therefore, the analgesic and anti-inflammatory effects induced by MAGL inhibition can be dependent on two underlying mechanisms, the first by directly increasing 2-AG levels and the second by lowering the arachidonic acid formation as previously described in brain [1]. Thus, MAGL could represent the link between two lipid signaling pathways: the endocannabinoid and the eicosanoid systems [11]. The modulation of MAGL activity can lead to several beneficial effects through either enhancing the tone of the endocannabinoid system or lowering eicosanoids production. Therefore, MAGL inhibitors may represent an

attractive therapeutic approach for the treatment of pain, inflammation, [12-15], anxiety [16,17], neurodegeneration [3,18,19], cancer [1,20] and other disorders [7-9].

Conventional assays to investigate the inhibition of MAGL employ the radioactive substrates [^{3}H]-2-AG or [^{3}H]-2-oleoyl glycerol (2-OG) [21-26], as well as the analytical determination of the arachidonic acid formation from 2-AG hydrolysis quantified by high-performance liquid chromatography (HPLC), mass spectrometry [6,27-29] or ultraviolet light (UV) [30,31]. Recently, a colorimetric assay that exploits 4-nitrophenylacetate (4-NPA) as non-specific chromogenic substrate for MAGL activity has been described [32]. In this assay, 4-NPA releases, upon hydrolysis, 4-nitrophenol (PNP), whose absorbance is measured at 405 nm. Thus, by quantifying the amount of absorbance, the assay enables monitoring the degree of MAGL activity. In addition, HPLC fluorescence assays have been developed exploiting 7-hydroxycoumarinyl arachidonate (7-HCA) [33] or 1,3-dihydroxypropan-2-yl 4-pyren-1-ylbutanoate [34] as substrates. In these two assays, the hydrolytic activity of MAGL is evaluated by the fluorimetric detection of 7-hydroxyl coumarin or 4-pyren-1-ylbutanoic acid formation, respectively.

In the present work, we show an alternative radioactive-free, sensitive and accurate HPLC-UV based method to evaluate MAGL activity and test new inhibitors. The assay is based on the chromatographic separation and subsequent absorbance measurement of PNP, that is formed upon hydrolysis of 4-NPA. This method (4-NPA method) enables measuring the PNP formation at the optimal wavelength of 315 nm avoiding the potential interference of any residual, non-cleaved 4-NPA which still exhibits a significant absorbance at such wavelength. Furthermore, the chromatographic separation of PNP before measuring the absorbance, prevents any interference in the assay readout potentially generated by coloured or fluorescent compounds. This allows to safely evaluate the inhibition of MAGL activity by

molecules which possess intrinsic absorbance property, that is for example a typical feature of many natural products.

We also investigated the validity of this method under different assay conditions that resemble the cellular environment of MAGL activity. The crystal structure of MAGL was recently resolved and it provided evidence that the catalytic activity occurs at the interface between the inner leaflet of the plasma membrane and the cytosol. First, the enzyme "recruits" the lipophilic substrates (e.g., 2-AG) from the membrane and then moves them to the active site where the hydrolysis takes place [35]. In order to reproduce *in vitro* this condition, we decided to perform additional experiments where the substrate is presented to the enzyme in a lipid/water interface. This was achieved through the addition of the surfactant Triton® X-100, as a micelle forming agent, in the assay buffer [34] and using the more lipophilic substrate, 4-nitrophenyldodecanoate (4-NPDo), whose hydrolysis generates PNP (4-NPDo/TX method). Although it is not specifically reported that MAGL can hydrolyse 4-NPDo, the latter is a well-known substrate for many other lipases.

2. Material and Methods

2.1 Chemicals and reagents

4-Nitrophenylacetate (4-NPA), 4-Nitrophenyldodecanoate (4-NPDo), 4-nitrophenol (PNP), Tris(hydroxymethyl)aminomethane (Tris base), Ethylenediaminetetraacetic acid (EDTA), Triton X-100, gradient grade solvents, acetonitrile (ACN) and methanol (MeOH), absolute ethanol, dimethylsulfoxide (DMSO), acetic acid and ammonium acetate for HPLC were purchased from Sigma-Aldrich. Benzyl [4-(5-methoxy-2-oxo-1,3,4-oxadiazol-3(2H)-yl]-2-methylphenyl)carbamate (CAY10499), 4-[Bis(1,3-benzodioxol-5-yl)hydroxymethyl]-1-piperidinecarboxylic acid 4-nitrophenyl ester (JZL184), 1,1,1,3,3,3-hexafluoropropan-2-yl-4-(3-phenoxybenzyl)piperazine-1-carboxylate (JW642), N-Methyl-N-[[3-(4-

pyridinyl)phenyl]methyl]-4'-(aminocarbonyl)[1,1'-biphenyl]-4-yl carbamic acid ester (WWL70), (3'-(aminocarbonyl)[1,1'-biphenyl]-3-yl)-cyclohexylcarbamate (URB597) and human recombinant MAGL (*hr*MAGL) were purchased from Cayman Chemicals. CAY10499, JZL184, JW642 WWL70 and URB597 stock solutions were prepared in DMSO or ethanol (according to Cayman product information) and then diluted in absolute ethanol in order to reach the desired concentration.

2.2 HPLC-UV chromatographic conditions

A Thermo Finnigan HPLC system was used to quantify PNP formed after enzymatic hydrolysis of both 4-NPA and 4-NPDo. The HPLC system consists of a Thermo Finnigan SpectraSystem SN4000 system controller, coupled with P2000 pump, a SCM1000 degasser and a UV2000 UV detector at operation wavelength of 270 nm (4-NPA and 4-NPDo) and 315 nm (PNP). Data were monitored and analyzed using ChromQuest software (Thermo Finnigan, Waltham, MA, USA). Separation of compounds was carried out at ambient temperature on to reverse-phase column (150 x 4.6 mm; 5 µm). The mobile phase, delivered at a flow rate of 1.0 ml/min, consists of methanol and ammonium acetate buffer (pH 4.0; 10 mM,) (53:47, v/v) for 4-NPA and PNP separation. For 4-NPDo and PNP separation, gradient conditions were used; solvent A was ACN and solvent B was ammonium acetate buffer (pH 4.0; 10 mM). Gradient conditions at a flow rate of 1.0 ml/min were as follows: 0-3 min linear gradient from 40% to 90% of A; 3-20 min. 90% of A. Ammonium acetate buffer was filtered through a 0.45 µm membrane before use. The sample injection volume was 20 µl.

2.3 Substrate stability

4-NPA stability was tested preparing a 4.25 mM solution in DMSO, Tris-HCl buffer (pH = 7.2; 10 mM containing 1.0 mM EDTA) or absolute ethanol and they were stored at room

temperature, 3 °C or -20 °C. Samples analysis was performed by diluting 10 µl of each stock solution in 170 µl of water and monitoring 4-NPA and PNP concentrations by HPLC after 5 h and 48 h.

4-NPDo stability was tested preparing a 486 µM solution in ACN in the same conditions above reported for 4-NPA.

2.4 Surface tension measurements

The measurements of surface tension for a concentration series of Triton® X-100 surfactant in Tris-HCl buffer solutions were performed using a DuNuoy tensiometer (K6, Kruss, Germany) equipped with a platinum ring (mean ring radius 9.545 mm and wire radius 0.185 mm). The surfactant concentrations analysed for buffer solution ranged between 0.3000 and 0.0005 % w/w and three replicates were carried out for each measurement.

2.5 HPLC-UV assay

For 4-NPA method, an aliquot of stock solutions of *hr*MAGL (10 µg/50 µl) was diluted 1:125 with Tris-HCl buffer (pH = 7.2; 10 mM, containing 1.0 mM EDTA) to obtain the working solutions of *hr*MAGL at 1.6 ng/µl. The stock and working solutions were stored at −20 °C.

In a 0.5 ml spin tube containing 75 µl of Tris-HCl buffer (pH= 7.2; 10 mM containing 1.0 mM EDTA), 5 µl of working solution *hr*MAGL (8 ng), 5 µl inhibitor (or solvent as control) were added. Samples were pre-incubated for 30 minutes at 37 °C and then 5 µl of a solution of 4-NPA in absolute ethanol (4.25 mM) were added. Samples were incubated for 10 minutes at 37 °C. The enzymatic reaction was stopped by cooling in an ice bath for 10 minutes and then 20 µl of the reaction mixture were taken and analysed by HPLC.

The evaluation of the initial velocity was carried out by incubating the samples at 37 °C at different times (0, 5, 15, 25, 35, and 45 minutes). In the reversibility assay a rapid 1:10 dilution of the pre-incubated mixture was performed before adding 4-NPA. Then, the reaction mixture was incubated at 37 °C for 10, 30 and 60 min. before quantifying PNP formation. The competition assay was performed by adding different concentrations of substrate (ranging from 0.05 to 4 mM) to the pre-incubated mixture and the enzyme activity was evaluated after 10 minutes at 37 °C.

Kinetics parameters (K_m and V_{max}) were calculated according to a procedure previously reported [32]. In a 0.5 ml spin tube containing 80 µL of Tris-HCl buffer (10 mM, pH = 7.2, containing 1.0 mM EDTA), 5 µL of working solution of *hr*MAGL (8 ng) and 5 µL of the proper solution of 4-NPA in ethanol (55 µM to 5000 µM) were added. Samples were incubated for 10 minutes at 37 °C and analysed by HPLC.

For 4-NPDo/TX method, an aliquot of a solution of *hr*MAGL (0.19 µg/µl) was diluted 1:120 with Tris-HCl buffer (pH = 7.2 10 mM containing 1 mM EDTA). In a 0.5 mL spin tube containing 80 µl of Tris-HCl buffer (10 mM, pH 7.2, containing 1.0 mM EDTA and 0.2 % (m/v) Triton® X-100), 5 µl of a solution of inhibitor (or solvent in case of the controls) and 5 µL of a solution of 4-NPDo in ACN (486 µM) were added. The mixture was pre-incubated for 10 minutes at 37 °C and then the enzymatic reaction was started by adding of 5 µL of the working solution of *hr*MAGL and continued for 30 min. at 37 °C. The final incubation volume of 90 µL contained 27 µM of the substrate and 8 ng of MAGL. The enzymatic reaction was stopped by cooling in ice bath and then 20 µl of the reaction solution were analyzed by HPLC.

Kinetics parameters (K_m and V_{max}) were calculated. First, regression progress curves of enzymatic reaction were obtained for different substrate concentrations (from 25 µM to 250 µM). In a 0.5 ml spin tube containing 80 µl of Tris-HCl buffer (pH 7.2, 10 mM, containing

189 1.0 mM EDTA and 0.2 % (m/v) Triton® X-100) 5 µl of the proper solution of 4-NPDo were
190 added. Samples were pre-incubated for 10 minutes at 37 °C and then 5 µL of the working
191 solution of *hr*MAGL (8 ng) were added. After further incubation at 37 °C for various times
192 (from 0 to 55 minutes), 20 µl of the reaction solution were analyzed by HPLC. The product
193 generated (PNP) was plotted versus times (X-axis) to generate the reaction progress curves
194 for each substrate concentration.

195 Initial velocity (v_o) for each regression progress curve is equivalent to the slope of the
196 linear portion of the curve and it was calculated using linear regression method. Then, the
197 resulting slope (initial velocity) for each of the reaction progress curves were plotted on the
198 Y-axis against the concentration of substrate (X-axis) by a nonlinear regression analysis,
199 using a rectangular hyperbola model to evaluate K_m and V_{max} using 4-NPDo as MAGL
200 substrate.

201

202 *2.6 Chromatographic method validation*

203 Calibration curve for 4-NPA and PNP were built by analysing triplicate of eight
204 concentrations for each substance (from 250 µM to 0.25 µM for PNP, from 125 µM to 25 µM
205 for 4-NPA). Since the separation of 4-NPDo and PNP has required novel chromatographic
206 conditions, the calibration curve for both the analytes was evaluated by analysing triplicate of
207 eight concentrations for each substance (from 125 µM to 0.25 µM). Limit of detection and
208 quantification were also evaluated.

209 Least squares regression parameters for the calibration curve were calculated, and the
210 concentrations of the test samples were interpolated from the regression parameters. Sample
211 concentrations were determined by linear regression, using the formula Y=mX+b, where
212 Y=peak area, X=concentration of the standard in nanograms per millilitre, m=the slope of the
213 curve and b=the intercept with y-axis. Correlation coefficients for each of the calibration

curves were >0.99. Accuracy and intermediate precision were determined on different analytes concentration levels: low (250 and 10.0 μM), medium (750 and 50 μM) and high QC (2000 and 100 μM) for 4-NPA, 4-NPDo and PNP, respectively. Accuracy and within-run and between-run precision were assessed on quality control samples (QC samples) and determined by replicate analysis using seven determinations of different concentration levels: low (0.5 mM), medium (50 mM) and high (100 mM) (Table 1).

For accuracy five replicates of each concentration was analysed during the same analytical session. Intermediate precision was tested analysing triplicates of each concentration in three different days.

2.7 Method validation

MAGL initial velocity was evaluated in order to define the best incubation time at 37 °C. K_m and V_{max} values of *hr*MAGL for 4-NPA and for 4-NPDo were evaluated to ensure a good precision of the method. For 4-NPA method, MAGL reference inhibitors CAY10499, JZL184 and JW642 were screened at 1 μM as well as WWL70, URB597 as negative controls. Applicability of the method was tested calculating the IC_{50} values of MAGL inhibitors and characterizing the JZL184 mechanism of inhibition. Inhibition curve experiments were performed evaluating a minimum of six different concentrations of each compound ranging from 1 μM to 67 pM for JZL184, from 7 μM to 0.7 nM for JW642 and from 5 μM to 50 pM for CAY10499. Data were collected from two independent experiments performed in triplicates.

In the case of 4-NPDo/TX method, JW642 and JZL184 were screened evaluating a minimum of six different concentrations from 1 nM to 150 μM.

2.8 Radiometric hrMAGL assay

*hr*MAGL esterase activity was assessed as previously reported [36]. The reaction consisted of 196 µl assay buffer (pH 7.4, 10 mM Tris-HCl, 1 mM EDTA, plus 0.1% fatty acid-free BSA) containing 25 ng of *hr*MAGL and 2 µl of JZL184, CAY10499, JW642 or vehicle. The mixture was incubated for 30 min at 37 °C and afterwards, 1.5 nM of [^{3}H]-2-oleoylglycerol ([^{3}H]-2OG) (2 µl) were added. The solution was further incubated for 20 min. at 37 °C and the reaction was stopped by adding 400 µl of chloroform:methanol mixture (1:1, v/v). Tubes were vortexed and centrifuged for 10 min. at 10 000 x g at 4 °C. Finally, the upper aqueous phase was transferred in scintillation tubes and mixed with 3 ml of Ultima Gold scintillation liquid (PerkinElmer Life Sciences). Radioactivity was measured using a Beckman LS6500 scintillation counter. Data were collected from two independent experiments performed in triplicates and the results were expressed as % [^{3}H]-glycerol formation, relative to that in vehicle-treated samples (=100%).

2.9 Data analysis

Results are expressed as mean values ± S.D. for each examined group. Statistical significance of differences between groups was determined by the Student's *t*-test (paired t-test) with GraphPad Prism 5 software (GraphPad Software Inc., San Diego, CA, USA). Statistical differences between treated and vehicle control groups were determined by Student's *t*-test for dependent samples. Differences between the analysed samples were considered as significant if $p \leq 0.05$.

3. Results

3.1. Chromatographic conditions optimization and validation

In order to assess MAGL activity by HLPC, we checked the chromatographic conditions to detect and quantify the hydrolytic product PNP from 4-NPA or from 4-NPDo (Fig. 1). A C18 stationary phase was used to perform resolution of analytes eluting with different mixture of methanol and ammonium acetate buffer for 4-NPA or ACN and ammonium acetate buffer for 4-NPDo. Different pH buffers (7, 6, 5 and 4) were tested obtaining a best resolution at acid pH due to the undissociated form of the PNP. A diode-array detector was used to record UV-visible spectra of each analytes at pH = 7 (pH condition for colorimetric assay) and pH = 4 (pH condition for chromatographic assay) highlighting a maximum absorbance at 270 nm for 4-NPA and 4-NPDo and at 315 nm for PNP (Fig. 2). UV-VIS spectra comparison showed a greater absorbance of PNP at the selected wavelength (315 nm) than that used for the colorimetric assay (405 nm) in both pH conditions. Method linearity was assessed by performing calibration curves of PNP. Quantification of PNP was performed at 315 nm. The calculated coefficient of determination for linear regression (R^2) was 0.999 for 4-NPA method and 0.998 for 4-NPDo/TX method and limit of quantification (LOQ) and detection (LOD) were 0.50 μM and 0.25 μM respectively for both methods.

3.2 Determination of critical micelle concentration (CMC)

The data obtained from surface tension measurements showed typical curves of surfactants, (Triton® X-100), i.e. in the first part the surface tension depends linearly on the logarithm of the concentration up to CMC; above this value it becomes independent of the concentration forming a plateau. The CMC was determined from the intersection between the regression straight line of the linearly dependent region and the straight line describing the plateau. The CMC value determined for surfactant solution was 0.0190 % w/w in Tris-HCl buffer.

3.3 Substrate stability

4-NPA stability was assessed in different solvents commonly used in biological assays, such as DMSO, ethanol and Tris-HCl buffer, with the latter also used for *hr*MAGL dilution. Different temperatures were tested to evaluate the best conditions for stock solution storage and substrate stability during the assay execution. Spontaneous hydrolysis was observed at room temperature and 3 °C in all the solvents excepted for the absolute ethanol which showed a negligible degradation at r.t. and 3 °C (Table 2). DMSO solutions stored at 3 °C, showed higher degradation of 4-NPA than the sample stored at r.t.. Such effect is probably a consequence of the freezing and thawing cycle of the DMSO solution which can enhance substrate degradation. For longer storage periods, the best conditions are represented by absolute ethanol as solvent and -20 °C as temperature (Table 2). Those conditions ensure a standard stability of the substrate for at least two months.

4-NPDo stability was tested in ACN in the same conditions above reported for 4-NPA. This substrate showed a negligible degradation at all different tested conditions (data not showed).

In every experiment a background analysis (without enzyme) of the spontaneous, non-specific cleavage of the substrate was included and it was always subtracted.

3.4 Method optimization and validation

In order to optimize the HPLC-UV based assay, the initial velocity of MAGL activity was evaluated for the two substrates (4-NPA and 4-NPDo) in order to define the reaction kinetics of both conditions. In case of 4-NPA, the data obtained showed that the rate of hydrolysis is linear in the first 20 minutes of incubation at 37 °C, therefore 10 minutes was chosen for testing the inhibitors.

Conversely, for 4-NPDo/TX method, a preincubation time of 10 min. of substrate and inhibitor in Tris-HCl buffer was chosen accordingly to that reported for a similar method using Triton® X-100 as a micelle forming agent [34]. Then the enzymatic reaction was started, the incubation was continued for 30 min., nevertheless kinetic experiments showed that the rate of hydrolysis is linear within the first 20 minutes. Because many inhibitors of MAGL act by forming covalent bonds with the enzyme, a somewhat longer incubation period was chosen to give the inhibitors enough time to exert their full activity.

In order to validate our assay, we calculated the Michaelis-Menten constant (K_m) and V_{max} for the enzymatic reaction, obtaining values corresponding to 0.50 ± 0.06 mM and 30.83 ± 1.29 μmol min^{-1} mg^{-1}, respectively for 4-NPA method. These parameters are in agreement with literature for the evaluation of MAGL activity carried out by exploiting the same 4-NPA/PNP principle in the colorimetric assay (K_m: 0.2 ± 0.05 mM and V_{max}: 52.2 ± 2.3 μmol min^{-1} mg^{-1}) [32].

In the case of 4-NPDo/TX method, the K_m and V_{max} values were 27 ± 1.3 μM and 1.2 ± 0.11 μmol min^{-1} mg^{-1} respectively, suggesting a more efficient enzymatic activity.

The 4-NPA method was further validated by testing the effect of conventional well characterized MAGL inhibitors such as JZL184, CAY10499 and JW642. As negative controls, the selective fatty acid amide hydrolase inhibitor URB597 and the ABHD-6 inhibitor WWL70 were also included. In a first attempt experiments were carried out at different pre-incubation times (from 0 to 30 min). The data confirmed a variability of JZL184 inhibitory activity at different times of pre-incubation as previously reported in literature [37]. As shown in Fig. 3 JZL184 exerted its maximal inhibition as early as after 20 min. of pre-incubation. A pre-incubation time of 30 min. was further applied to screen all the inhibitors which were initially tested at 1 μM. The results confirmed the strong inhibitory activity of JZL184, CAY10499 and JW642 and the inactivity of URB597 and WWL70 (Fig.

4). The method was further validated by building concentration-dependent inhibition curves for JZL184, CAY10499 and JW642 which showed IC_{50} values of 24.17 ± 1.16 nM, 216.0 ± 2.66 nM and 7.43 ± 1.08 nM, respectively. The data were compared with IC_{50} values obtained by performing the classic radiometric assay. As shown in Table 3, no significant differences were observed among the two sets of values. IC_{50} values of JW642 are fully in agreement with literature [38], while the values calculated for CAY10499 are slightly, but likely not significantly lower than the one reported in literature [32]. IC_{50} values of JZL184 are fully in agreement with literature for both methods since it was already reported that JZL184 shows a reduced potency to inhibit MAGL activity when this was assessed by the colorimetric 4NPA/PNP method compared to the radioactive-based assay [37].

The 4-NPA method was also tested whether it would be suitable for characterizing the mechanism of enzymatic inhibition (reversibility and competitiveness). JZL184 was selected as reference compound. Reversibility assays were performed by a 10x dilution of the pre-incubated samples before adding 4-NPA and the recovery of *hr*MAGL activity over time was monitored. The results confirmed the stability of the covalent interaction enzyme-JZL184 highlighting an irreversible mode of inhibition (Fig. 5), according to literature [29].

Michelis-Menten kinetics assay was used to confirm the non-competitive interaction of JZL184 with the enzyme. The results showed a decrease in the V_{max} (61.42 ± 5.9 μmol min^{-1} mg^{-1} and 44.41 ± 4.3 μmol min^{-1} mg^{-1} for control and JZL184, respectively) but no changes in the K_m values upon JZL184 treatment (1.08 ± 0.26 mM and 1.47 ± 0.36 mM for control and JZL184, respectively) (Fig. 6). Thus, those data confirmed the non-competitive behaviour of this compound in *hr*MAGL inhibition [29].

In case of the 4-NPDo/TX method, JW642 and JZL184 were used as positive controls for MAGL inhibition and they showed IC_{50} values of 107.54 ± 11.3 nM and 145.67 ± 12.5 nM, respectively. In comparison with the 4-NPA method, the inhibitors showed a slight loss of

potency as it was also reported for a similar method using Triton® X-100 as micelle forming agent [34].

4. Discussion

MAGL is the main hydrolytic enzyme for 2-AG and exerts a tight control of the endogenous levels of this lipid mediator. Many lines of evidence showed that inhibition of MAGL leads to a massive increase of 2-AG especially in the brain [9]. Recently, other two enzymes, ABHD-6 and -12 have been identified as hydrolytic enzymes for 2-AG [5, 6]. Their contribution on the total 2-AG cleavage can be mild (up to 20%) in case of the simultaneous presence of MAGL (like in neurons) or very consistent in case of the absence of MAGL, as it has been recently described for certain lines of macrophage [39]. Therefore, it is of high importance to characterize 2-AG hydrolysis inhibitors for the impact on the single enzymes involved in such process. The commonly used assays to evaluate 2-AG hydrolysis are based on radiolabelled isotope substrate, bulky fluorescent substrate or by using very sensitive and expensive analytical methods (i.e. LC-MS) which are not perfectly suitable for screening purposes. Few years ago a quick and cheap assay for the detection of MAGL activity by using 4-NPA as substrate was developed [32]. In the assay 4-NPA is hydrolysed and releases 4-nitrophenol (PNP), which has an absorption in the UV-visible range (as well as a lot of nitro derivatives), thus making the test suitable to perform medium throughput screening for MAGL inhibitors in 96 and 384-well plate format. Despite the assay is easy to perform, the sensitivity of the detection is not optimal due to the range of wavelength (405-415 nm) used to quantify PNP formation. In fact, the optimum UV-visible absorption peak for PNP is at λ=315 nm with only a low absorption at $\lambda \geq 400$ nm (see Fig. 2). Changing the wavelength of detection would raise another experimental issue because the non-cleaved 4-NPA, which has an absorption peak at λ=270 nm, still exhibits a significant absorption in the range of 300-320

386 nm thus potentially interfering with the quantification of the hydrolytic product PNP (see Fig.
387 2).

388 Here we describe an implemented version of the 4-NPA/PNP assay by applying a HPLC
389 separation step before quantifying the absorbance of the hydrolytic product. The use of the
390 chromatographic system combined with an optimal UV-visible wavelength ensures a high
391 sensitivity and specificity of the PNP detection as well as a significant reproducibility and
392 accuracy of the results as confirmed by the data obtained testing different MAGL inhibitors
393 (see Table 3). The chromatographic separation of the hydrolytic product from the rest of the
394 reaction mixture before performing the absorbance measurement ensures that PNP can be
395 quantified at its optimal wavelength of absorption (315 nm) preventing any potential
396 interference of some residual, non-cleaved 4-NPA. The 4-NPA method was validated in
397 comparison to the benchmark radioactive-based assay currently used to evaluate MAGL
398 activity. The IC_{50} values calculated for some well-characterized potent and selective MAGL
399 inhibitors by using the classical radiometric assay were not significantly different from the
400 values calculated with the HPLC-UV method. Moreover, this HPLC-UV assay was
401 successfully applied to test the mechanism of MAGL inhibition showing that this method is
402 suitable to assess the reversible/irreversible enzyme-inhibitor interaction and the behaviour of
403 the compound in relation to the catalytic site and the substrate (competitive/non-competitive).

404 In addition, we showed that our method is also suitable for testing inhibitors using assay
405 conditions which resemble the physiological environment of MAGL activity that occurs at
406 the interface between the cell membrane and the cytosol. As described in the method section,
407 we used the surfactant Triton® X-100 to form micelles and 4-NPDo as lipophilic MAGL
408 substrate. Our data showed that in these conditions the enzymatic reaction is more efficient
409 than using 4-NPA as substrate. On the other hand, the potency of the tested inhibitors
410 determined by the 4-NPDo/TX method was lower than using the 4-NPA method (in absence

411 of Triton® X-100). These results are not totally unexpected since in a similar HPLC-based
412 method it was already reported that Triton® X-100 reduces the potency of enzyme inhibitors
413 [34]. This also confirms that inhibition potencies can significantly vary depending on the
414 assay conditions such as concentration of the substrate, presence of additives, and incubation
415 time.

416 The HPLC-UV methods here described are not probably the most suitable format for a
417 medium/high throughput screening but the use of chromatographic separation of the substrate
418 (4-NPA or 4-NPDo) and the product (PNP) achieves a high standard of selectivity for the
419 detection of the analytes with a negligible overlap in the UV measurements. This also
420 prevents, in an unequivocal manner, any interference related to the intrinsic absorbance of
421 screened compounds or metabolites generated upon enzymatic cleavage which could affect
422 the final readout of the assay. This issue is of particular importance when natural products are
423 tested. Recently, several natural compounds have been identified and characterized as MAGL
424 inhibitors such as the triterpenes β-amyrin, euphol and pristimerin [36,40,41], with the latter
425 being the most potent inhibitor with an IC_{50} value of 93 nM [41]. Pristimerin has an intense
426 orange-yellow colour with an absorption peak at λ=420 nm and a significant absorption
427 already at λ=320-340 nm [42]. Therefore, pristimerin interferes strongly or weakly,
428 depending on the concentration with the quantification of PNP either at λ=405 nm (the
429 wavelength suggested for the colorimetric quantification assay) or λ=315 nm (the optimal
430 peak of absorption of PNP). Several classes of molecules and chemical scaffolds possess
431 intrinsic absorption or fluorescent properties which can seriously affect the quantification of
432 PNP absorbance. For example, flavonoids consist of a large group of polyphenolic
433 compounds having a benzo-γ-pyrone structure which are ubiquitously present in plants and
434 are responsible for the variety of pharmacological activities. Quercetin, kaempferol and
435 luteoline are among the most studied members of this class of compounds [43]. All three

molecules show an absorption peak in the range of 250 nm<λ<450 nm, which may interfere with many absorbance/fluorescence based biological assays. The same issue is present with diarylheptanoids, of which curcumin is the most important bioactive representative [44]. Curcumin has a strong intrinsic absorbance with λ_{max} ranging from 400 to 550 nm, depending of the solvent [45]. Polyphenols are another common natural source of bioactive compounds. For example, *trans*-resveratrol has an absorption peak at λ=300-320 nm, leading to potential alterations of any colorimetric UV-visible detection based assay [46].

By applying the HPLC-UV method, the chromatographic separation of the hydrolytic product from the substrate and the tested inhibitors avoids any interference in the quantification of the PNP absorption allowing an accurate, specific and unbiased result.

Finally, the low specificity of 4-NPA as a substrate for esterase could be exploited by our HPLC-UV method to characterize the effect of compounds not only on MAGL activity, but also towards the recently identified 2-AG hydrolytic enzymes ABHD-6 and ABHD-12, for which the pharmacological repertoire of inhibitors is still not satisfying. Only very recently some compounds have been characterized as selective and potent inhibitors of ABHD-6, such as the carbamate WWL70 and piperidyl-1,2,3-triazole ureas [5,47], while no potent and selective inhibitor for ABHD-12 has been described so far.

5. Conclusion

The developed HPLC assays represent an implemented versions of the "classical" 4-NPA-PNP procedure: indeed the metabolite concentration is determined after chromatographic separation. This alternative approach allows to obtain an high sensitivity and to check the activity towards MAGL of compounds/mixture characterized by high absorbance in the UV-visible range, avoiding the use of radioactive substrate. Therefore these

methods may represent an helpful tool in the identification/discovery of new natural/synthetic MAGL inhibitors.

Acknowledgements

This work was supported by National Interest Research Projects (PRIN 2010-2011, Grant 20105YY2HL_008).

References

[1] D.K. Nomura, D.P. Lombardi, J.W. Chang, S. Niessen, A.M. Ward, J.Z. Long, H.H. Hoover, B.F. Cravatt, Monoacylglycerol lipase exerts dual control over endocannabinoid and fatty acid pathways to support prostate cancer, Chem. Biol., 18 (2011) 846-856.

[2] P. Chanda, Y. Gao, L. Mark, J. Btesh, B. Strassle, P. Lu, M. Piesla, M. Zhang, B. Bingham, A. Uveges, D. Kowal, D. Garbe, E.V. Kouranova, R.H. Ring, B.Bates, M.N. Pangalos , J.D. Kennedy, G.T. Whiteside, T.A. Samad, Monoacylglycerol lipase activity is a critical modulator of the tone and integrity of the endocannabinoid system, Mol. Pharmacol., 78 (2010) 996-1003.

[3] J. Schlosburg, J. Blankman, J. Long, D. Nomura, B. Pan, S. Kinsey, P. Nguyen, D. Ramesh, L. Booker, J. Burston, E.A. Thomas, D.E. Selley, L.J. Sim-Selley, Q.S. Liu, A.H. Lichtman, B.F. Cravatt, Chronic monoacylglycerol lipase blockade causes functional antagonism of the endocannabinoid system, Nat. Neurosci., 13 (2010) 1113-1119.

[4] E. Sigel, R. Baur, I. Rácz, J. Marazzi, T. Smart, A. Zimmer, J. Gertsch, The major central endocannabinoid directly acts at GABA(A) receptors, Proc. Natl. Acad. Sci. U S A, 108 (2011) 18150-18155.

[5] W.R. Marrs, J.L. Blankman, E.A. Horne, A. Thomazeau, Y.H. Lin, J. Coy, A.L. Bodor, G.G. Muccioli, S. Hu, G. Woodruff, S. Fung, M. Lafourcade, J.P. Alexander, J.Z. Long, W. Li, C. Xu, T. Möller, K. Mackie, O.J. Manzoni, B.F. Cravatt, N. Stella, The serine hydrolase ABHD6 controls the accumulation and efficacy of 2-AG at cannabinoid receptors, Nat. Neurosci., 8 (2010) 951-957.

[6] J.L. Blankman, G.M. Simon e B.F. Cravatt, A comprehensive profile of brain enzymes that hydrolyze the endocannabinoid 2-arachidonoylglycerol, Chem Biol. 12 (2007) 1347-1356.

[7] S. Saario, J. Laitinen, Therapeutic potential of endocannabinoid-hydrolysing enzyme inhibitors, Basic Clin. Pharmacol. Toxicol., 101 (2007) 287-293.

[8] J. Schlosburg, S. Kinsey A. Lichtman, Targeting fatty acid amide hydrolase (FAAH) to treat pain and inflammation, AAPS J., 11 (2009) 39-44.

[9] J. Long, W. Li, L. Booker, J. Burston, S. Kinsey, J. Schlosburg, F. Pavón, A. Serrano, D. Selley, L. Parsons, A. Lichtman B. Cravatt, Selective blockade of 2-arachidonoylglycerol hydrolysis produces cannabinoid behavioral effects, *Nat. Chem. Biol.,* 5 (2009) 37-44.

[10] S. Kinsey, S. O'Neal, J. Long, B. Cravatt, A. Lichtman, Inhibition of endocannabinoid catabolic enzymes elicits anxiolytic-like effects in the marble burying assay, Pharmacol. Biochem. Behav., 98 (2011) 21-27.

[11] M. M. Mulvihill e D. K. Nomura, «Therapeutic potential of monoacylglycerol lipase inhibitors,» *Life Sciences,* vol. 92, pp. 492-497, 2013.

[12] J. Guindon, A. Hohmann, The endocannabinoid system and cancer: therapeutic implication, Br. J. Pharmacol., 163 (2011)1447-1463.

[13] S. Kinsey, J. Long, S. O'Neal, R. Abdullah, J. Poklis, D. Boger, B. Cravatt, A. Lichtman, Blockade of endocannabinoid-degrading enzymes attenuates neuropathic pain, J. Pharmacol. Exp. Ther., 330 (2009) 902-910.

[14] J. Long, D. Nomura, R. Vann, D. Walentiny, L. Booker, X. Jin, J. Burston, L. Sim-Selley, A. Lichtman, J. Wiley, B. Wiley, B. Cravatt, Dual blockade of FAAH and MAGL identifies behavioral processes regulated by endocannabinoid crosstalk in vivo, Proc. Natl. Acad. Sci. U S A, 106 (2009) 20270-20275.

[15] M. Alhouayek, D. Lambert, N. Delzenne, P. Cani, G. Muccioli, Increasing endogenous 2-arachidonoylglycerol levels counteracts colitis and related systemic inflammation, FASEB J., 25 (2011) 2711-2721.

[16] N. Sciolino, W. Zhou, A. Hohmann, Enhancement of endocannabinoid signaling with JZL184, an inhibitor of the 2-arachidonoylglycerol hydrolyzing enzyme monoacylglycerol lipase, produces anxiolytic effects under conditions of high environmental aversiveness in rats, Pharmacol. Res., 64 (2011), 226-234.

[17] J. Sumislawski, T. Ramikie, S. Patel, Reversible gating of endocannabinoid plasticity in the amygdala by chronic stress: a potential role for monoacylglycerol lipase inhibition in the prevention of stress-induced behavioral adaptation, Neuropsychopharmacology, 36 (2011) 2750-2761.

[18] D. Nomura, B. Morrison, J. Blankman, J. Long, S. Kinsey, M. Marcondes, A. Ward, Y. Hahn, A. Lichtman, B. Conti, B. Cravatt, Endocannabinoid hydrolysis generates brain prostaglandins that promote neuroinflammation, Science, 334 (2011) 809-813.

[19] J. Piro, D. Benjamin, J. Duerr, Y. Pi, C. Gonzales, K. Wood, J. Schwartz, D. Nomura, T. Samad, A dysregulated endocannabinoid-eicosanoid network supports pathogenesis in a mouse model of Alzheimer's disease, Cell Rep., 1 (2012) 617-623.

[20] L. Ye, B. Zhang, E. Seviour, K. Tao, X. Liu, Y. Ling, J. Chen, G. Wang, Monoacylglycerol lipase (MAGL) knockdown inhibits tumor cells growth in colorectal cancer, Cancer Lett., 301 (2011) 617-625.

534 [21] T. Dinh, D. Carpenter, F.M. Leslie, T.F. Freud, I. Katona, S.L. Sensi, S. Kathuria, D.
535 Piomelli, Brain monoglyceride lipase participating in endocannabinoid inactivation, PNAS,
536 99 (2002) 10819-10824.
537 [22] N. Ghafouri, N. Tiger, R. Razdan, A. Mahadevan, R. Pertwee, B. Martin, C.J. Fowler,
538 Inhibition of monoacylglycerol lipase and fatty acid amide hydrolase by analogues of 2-
539 arachidonoylglycerol, Br. J. Pharmacol., 143 (2004) 774-784.
540 [23] J. Brengdahl, C. Fowler, A novel assay for monoacylglycerol hydrolysis suitable for
541 high-throughput screening, Anal. Biochem., 359 (2006) 40-44.
542 [24] G. Ortar, M. Cascio, A. Moriello, M. Camalli, E. Morera, M. Nalli, V. Di Marzo,
543 Carbamoyl tetrazoles as inhibitors of endocannabinoid inactivation: a critical revisitation.,
544 Eur. J. Med. Chem., 43, (2008) 62-72.
545 [25] T. Bisogno, G. Ortar, S. Petrosino, E. Morera, E. Palazzo, M. Nalli, S. Maione, V. Di
546 Marzo, Development of a potent inhibitor of 2-arachidonoylglycerol hydrolysis with
547 antinociceptive activity in vivo, Biochimica et Biophysica Acta, 1791 (2009) 53-60.
548 [26] S. Vandevoorde, B. Saha, A. Mahadevan, R. Razdan, R. Pertwee, B. Martin, C. Fowler,
549 Influence of the degree of unsaturation of the acyl side chain upon the interaction of
550 analogues of 1-arachidonoylglycerol with monoacylglycerol lipase and fatty acid amide
551 hydrolase, Biochem. Biophys. Res. Commun., 337 (2005) 104-109.
552 [27] A.R. King, A. Duranti, A. Tontini, S. Rivara, A. Rosengarth, J. Clapper, G. Astarita, D.
553 Piomelli, URB602 Inhibits Monoacylglycerol Lipase and Selectively Blocks 2-
554 Arachidonoylglycerol Degradation in Intact Brain Slices, Chem. Biol., 12, (2007) 1357-1365.
555 [28] A. King, A. Lodola, C. Carmi, J. Fu, M. Mor, D. Piomelli, A critical cysteine residue in
556 monoacylglycerol lipase is targeted by a new class of isothiazolinone-based enzyme
557 inhibitors, Br. J. Pharmacol., 157 (2009) 974-983.

558 [29] J.Z. Long, W. Li, L. Booker, J.J. Burston, S.G. Kinsey, J.E. Schlosburg, F.J. Pavón,
559 A.M. Serrano, D.E. Selley, L.H. Parsons, A.H. Lichtman, B. F. Cravatt, Selective blockade of
560 2-arachidonoylglycerol hydrolysis produces cannabinoid behavioral effects, Nat. Chem.
561 Biol., 5 (2009) 37-44.
562 [30] S.M. Saario, J.R. Savinainen, J.T. Laitinen, T. Järvinen R. Niemi, Monoglyceride lipase-
563 like enzymatic activity is responsible for hydrolysis of 2-arachidonoylglycerol in rat
564 cerebellar membranes, Bioch. Pharm., 67 (2004) 1381-1387.
565 [31] S. Saario, O. Salo, T. Nevalainen, A. Poso, J. Laitinen, T. Järvinen, R. Niemi,
566 Characterization of the sulfhydryl-sensitive site in the enzyme responsible for hydrolysis of
567 2-arachidonoyl-glycerol in rat cerebellar membranes, Chem Biol., 12 (2005) 649-656.
568 [32] G.G. Muccioli, G. Labar, D.M. Lambert, CAY10499, a Novel Monoglyceride Lipase
569 Inhibitor Evidenced by an Expeditious MGLAssay, ChemBioChem, 9 (2008) 2704-2710.
570 [33] Y. Wang, P. Chanda, P. Jones, J.D. Kennedy, A fluorescence-based assay for
571 monoacylglycerol lipase compatible with inhibitor screening, Assay Drug Dev. Technol., 6
572 (2008) 387-393.
573 [34] A. Holtfrerich, T. Makharadze, M. Lehr, High-performance liquid chromatography
574 assay with fluorescence detection for the evaluation of inhibitors against human recombinant
575 monoacylglycerol lipase, Analytical Biochemistry, 399 (2010) 218-224.
576 [35] G. Labar, C. Bauvois, F. Borel, J.L. Ferrer, J. Wouters, D.M. Lambert, Crystal structure
577 of the human monoacylglycerol lipase, a key actor in endocannabinoid
578 signaling,Chembiochem. 11 (2010) 218-227.
579 [36] A. Chicca, J. Marazzi, J. Gertsch, The antinociceptive triterpene β-amyrin inhibits 2-
580 arachidonoylglycerol (2-AG) hydrolysis without directly targeting cannabinoid receptors, Br.
581 J. Pharmacol., 167, (2012) 15906-15608.

582 [37] E. Björklund, E. Norén, J. Nilsson, C. Fowler, Inhibition of monoacylglycerol lipase by
583 troglitazone, N-arachidonoyl dopamine and the irreversible inhibitor JZL184: comparison of
584 two different assays, Br. J. Pharmacol., 161 (2010) 1512-1526.
585 [38] J.W. Chang, M.C. Niphakis, K.M. Lum, A.B. Cognetta, C. Wang, M.L. Matthews, S.
586 Niessen, M.W. Buczynski, L.H. Parsons, B.F. Cravatt, Highly Selective Inhibitors of
587 Monoacylglycerol Lipase Bearing a Reactive Group that Is Bioisosteric with
588 Endocannabinoid Substrates, Chem. Biol., 19 (2012) 579-588.
589 [39] M. Alhouayek, J. Masquelier, P. Cani, D. Lambert, G. Muccioli, Implication of the anti-
590 inflammatory bioactive lipid prostaglandin D2-glycerol ester in the control of macrophage
591 activation and inflammation by ABHD6, Proc. Natl. Acad. Sci. U S A, 110 (2013) 17558-
592 17563.
593 [40] J. Gertsch, R. Pertwee, V. Di Marzo, Phytocannabinoids beyond the Cannabis plant - do
594 they exist?, Br. J. Pharmacol., 160 (2010) 523-529.
595 [41] A. King, E. Dotsey, A. Lodola, K. Jung, A. Ghomian, Y. Qiu, J. Fu, M. Mor, D.
596 Piomelli, Discovery of potent and reversible monoacylglycerol lipase inhibitors, Chem. Biol.,
597 16 (2009) 1045-1052.
598 [42] P.K. Grant, A.W. Johnson, Pristimerin. Part I. The nature of the chromophore, J. Chem.
599 Soc., (1957) 4079-4089.
600 [43] S. Kumar, A.K. Pandey, Chemistry and biological activities of flavonoids: an overview,
601 ScientificWorld Journal, 2013 (2013) 1-16.
602 [44] K. Venugopala, V. Rashmi, B. Odhav, Review on natural coumarin lead compounds for
603 their pharmacological activity, Biomed. Res. Int. 2013, (2013) 1-14.
604 [45] C. Chignell, P. Bilskj, K. Reszka, A. Motten, R. Sik, T. Dahl, Spectral and
605 photochemical properties of curcumin, Photochem. Photobiol., 59, (1994) 3 295-302.

606 [46] L. Camont, C. Cottart, Y. Rhayem, V. Nivet-Antoine, R. Djelidi, F. Collin, J. Beaudeux,
607 D. Bonnefont-Rousselot, Simple spectrophotometric assessment of the trans-/cis-resveratrol
608 ratio in aqueous solutions, Anal. Chim. Acta, 634 (2009) 121-128.
609 [47] K. Hsu, K. Tsuboi, J. Chang, L. Whitby, A. Speers, H. Pugh, B. Cravatt, Discovery and
610 optimization of piperidyl-1,2,3-triazole ureas as potent, selective, and in vivo-active
611 inhibitors of α/β-hydrolase domain containing 6 (ABHD6), J. Med. Chem., 56 (2013) 8270-
612 8279.
613
614
615
616
617
618

Footnotes

[a] 4-NPA stability assessed in different solvents, at different temperatures and times of storage. Values are expressed as % of degraded 4-NPA.

[b] IC_{50} values of MAGL inhibitors obtained by the classical [^{3}H]-radiometric-based assay and the new HPLC-UV-based assay. Values are expressed as mean ± S.D., N= 9 from three independent experiments.

Tables:

Table 1. Accuracy and precision for PNP

***p*-nitrophenol concentration (μM)**	**Accuracy**		**Precision**			
	4-NPA method	**4-NPDo/TX method**	**4-NPA method**		**4-NPDo/TX method**	
			Within-run	**Between-run**	**Within-run**	**Between-run**
100	98.1±2.0	96.3±1.2	4.26	2.42	4.31	3.15
50	101.2±1.3	102.1±1.1	3.91	1.11	3.88	1.21
0.5	104.9±4.8	106.5±3.2	5.13	4.53	5.22	4.63

Table 2. 4-NPA stability.[a]

% of degraded 4-NPA after 5 h				% of degraded 4-NPA after 48 h			
	DMSO	Ethanol	Tris-HCl		DMSO	Ethanol	Tris-HCl
r.t.	2	1	60	r.t.	5	6	95
+3 °C	7	0	53	+3 °C	6	2	91
-20 °C	0	0	5	-20 °C	3	0	58

Table 3. IC_{50} values of MAGL inhibitors.[b]

Compounds	HPLC-UV-based assay (nM)	[^{3}H]-Radiometric-based assay (nM)
JZL184	24.2 ± 1.2	8.1 ± 5.2
CAY10499	216.0 ± 2.7	157.7 ± 42.9
JW642	7.43 ± 1.1	9.65 ± 3.5

Figures:

Fig. 1.

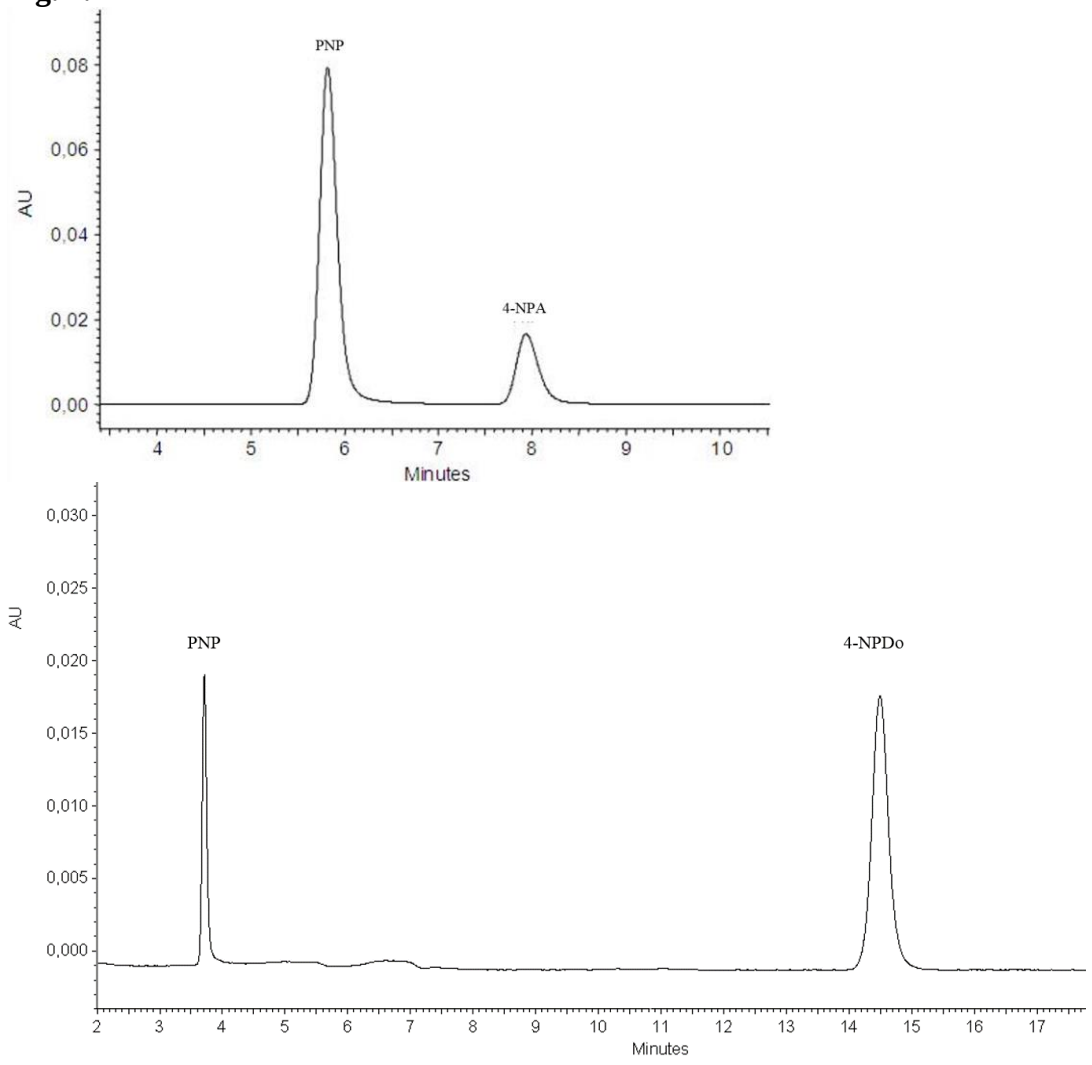

Fig.2.

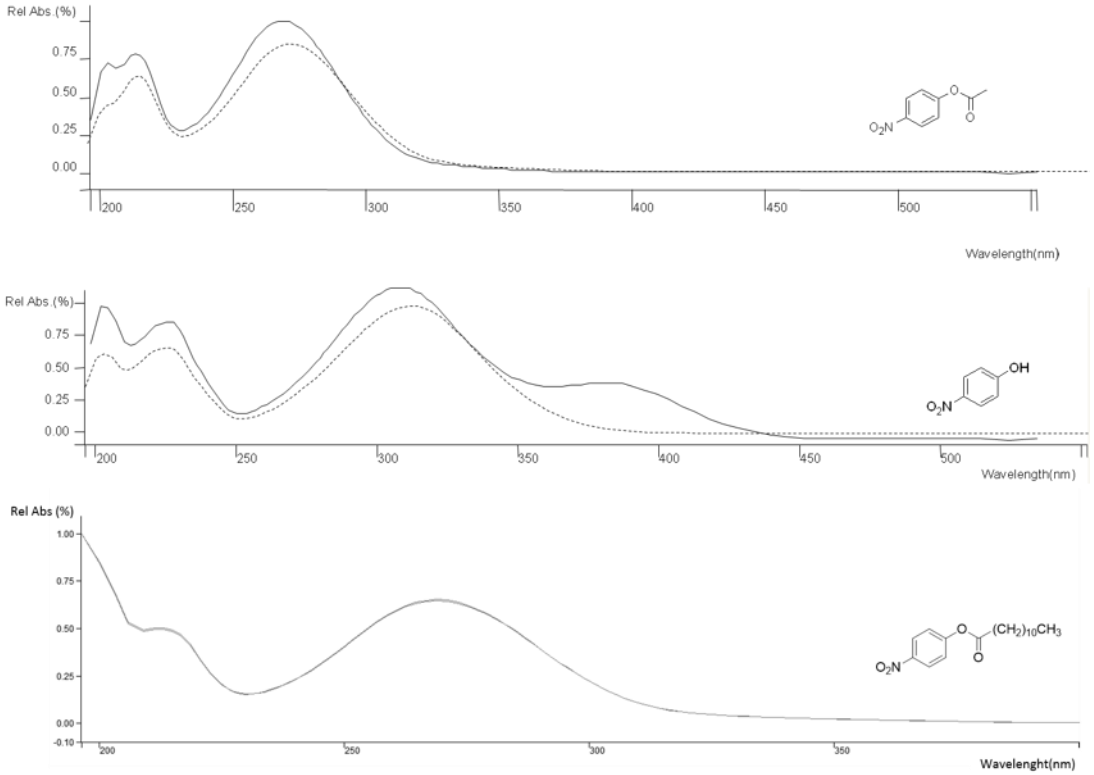
Rel Abs.(%)
0.75
0.50
0.25
0.00
200
250
300
350
400
450
500
Wavelength(nm)
O_2N
O
O
Rel Abs.(%)
0.75
0.50
0.25
0.00
200
250
300
350
400
450
500
Wavelength(nm)
OH
O_2N
Rel Abs (%)
1.00
0.75
0.50
0.25
0.00
-0.10
200
250
300
350
Wavelenght(nm)
O_2N
O
O
$(CH_2)_{10}CH_3$

Fig. 3.

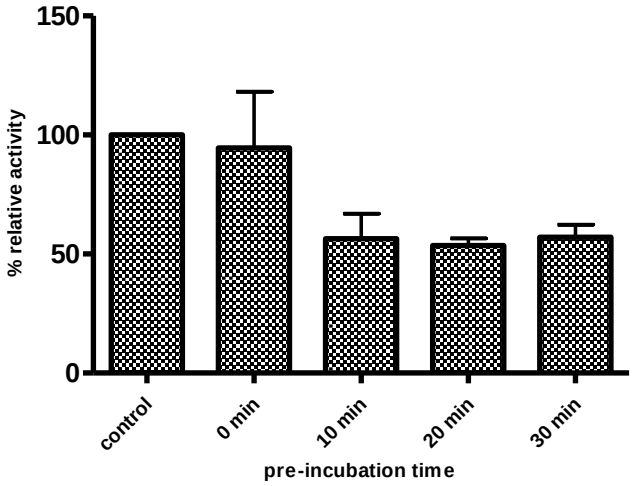
150
100
50
0
% relative activity
control
0 min
10 min
20 min
30 min
pre-incubation time

Fig.4.

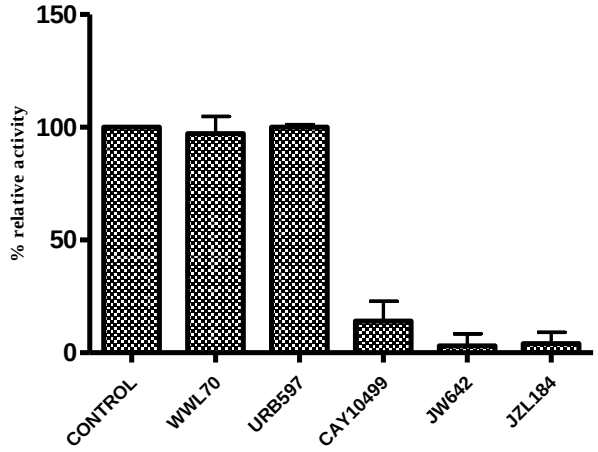

Fig. 5.

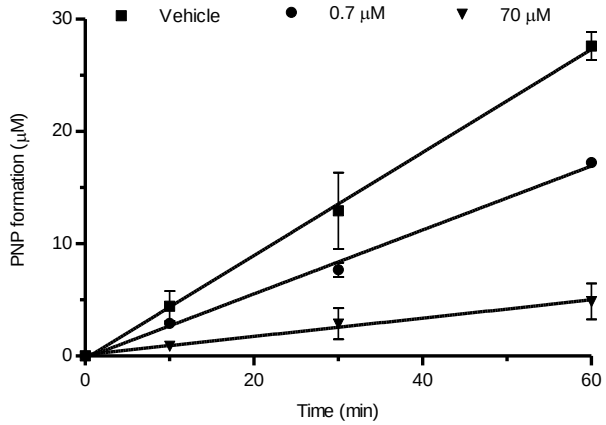

Fig. 6.

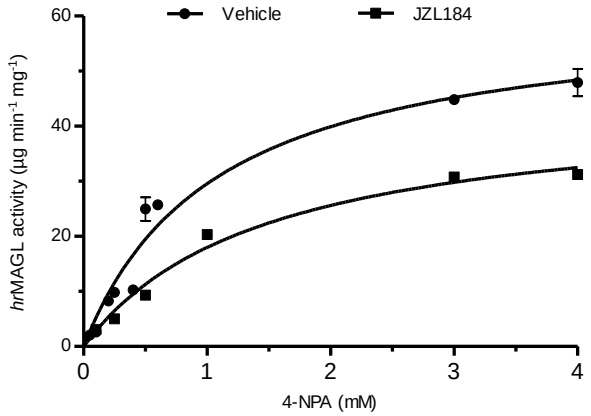

Figure legends:

Fig 1. Chromatograms of 4-NPA and PNP and of 4-NPDo and PNP at 315 nm performed at pH = 4.

Fig 2. UV absorption spectrum of 4-NPA and PNP at pH = 4 (dashed line) and at pH = 7 (solid line) and UV absorption spectrum of 4-NPDo at pH = 4.

Fig. 3. Influence of different pre-incubation times on JZL184 potency in inhibiting MAGL activity. JZL184 was assessed at the concentration of 33 nM. Values are expressed as mean ± S.D., N = 6 from two independent experiments

Fig. 4. Inhibition of *hr*MAGL activity by selective MAGL inhibitors (JZL184, CAY10499 and JW642) and negative controls (URB597 and WWL70). All the inhibitors were tested at the concentration of 1 µM. Values are expressed as mean ± S.D, N = 9 from three independent experiments.

Fig. 5. Reversibility of *hr*MAGL inhibition by JZL184. Rapid dilution assay of *hr*MAGL in the presence of JZL184 or vehicle. Results are expressed as amount of product generated (expressed as concentration). Values are expressed as mean ± S.D., N = 6 from two independent experiments.

Fig. 6. Michaelis-Menten analysis of *hr*MAGL reaction. Enzymatic activity was measured as µg min^{-1} mg^{-1} protein in the presence of vehicle (circles) or JZL184 33 nM (squares). Values are expressed as mean ± S.D., N = 6 from two independent experiments.